Journal of Theoretical and Applied Information Technology
15th December 2024. Vol.102. No. 23

ISSN: 1992-8645 www.jatit.org E-ISSN: 1817-3195

ADVANCED INSAR TECHNIQUES FOR LANDSLIDE DETECTION AND RISK ASSESSMENT: A CASE STUDY OF THE TAZA-AL HOCEIMA EXPRESSWAY IN MOROCCO

ISHAK HBIAK[1], OMAR BACHIR ALAMI[2], ANOUAR KESMAT[3], NIA MAJDA[4], SAID RHOUZLANE[5], MERIEM HABIBELLAH[6]

[1,2]Hassania School of Public Works, Systems Engineering Laboratory, Research Team SGEO, Morocco

[3]Consulting, Engineering and Development (CID), Department of Transportation, Morocco

[1,4,6]Hassania School of Public Works, Department of Bridges, Roads and Transport, Morocco

[5]Polytechnique Montréal, Department of Civil, Geological and Mining Engineering, Canada

E-mail: [1]ishak.hbiak@gmail.com / ishak.hbiak@ehtp.ac.ma, [2]alami@ehtp.ac.ma, [3]akesmat@cid.ma, [4]niamajda01@gmail.com, [5]said.rhouzlane@polymtl.ca, [6]habibellahmeriem@gmail.com,

ABSTRACT

The Taza-Al Hoceima expressway is a vital infrastructure that facilitates the integration of the region into Morocco's economic dynamics. Several challenges related to the difficult geotechnical context of the northern region arose during the construction period, and additional challenges continue to emerge concerning the sustainability of this infrastructure. Indeed, the complex geology and topography of the Taza province make it prone to land movements, posing risks to critical infrastructure. The objective of this study is to employ advanced Interferometric Synthetic Aperture Radar (InSAR) techniques to detect, monitor, and measure land movements, particularly landslides, along the infrastructure, using Sentinel-1 radar data covering the period from 2015 to 2020. Our work also focuses on explaining the instability movements measured during the study period by identifying their main causative factors. The study's findings also enable the identification of certain high-risk instability zones within our geologically complex study area, which require long-term monitoring.

Keywords: *Geotechnics, Remote sensing, Landslide, Synthetic Aperture Radar, PCA*

1. INTRODUCTION

Land movements in general, and slope movements and landslides in particular, constitute a major civil engineering and geotechnical challenge for infrastructure development and population safety. These events, often triggered by natural factors such as intense precipitation, earthquakes, or tectonic movements, can have dramatic consequences, including: significant material damage (destruction of road infrastructure, housing, water and electricity networks), human losses (direct victims of landslides or accidents related to traffic on damaged roads) and significant socio-economic impacts (interruption of road traffic, difficulties accessing disaster areas, disruption of economic activities) [1] [2].

In terms of landslide typology, we can cite: rockfall (the collapse of a rock mass due to its own weight or a load at its summit), creep (it occurs in loose soils subjected to a significant load causing soil creep, a slow and progressive slide), planar landslide following a straight rupture line, circular landslide (it occurs around a central axis at the rupture surface) and mudflow (it is a rapid flow of mud mixed with water, often caused by extreme precipitation or snowmelt).

Land and slope movements can have different causes: erosion and infiltration, faults/fractures, earthquakes, water saturation, or anthropogenic factors through earthworks. The main reinforcement techniques to strengthen slopes and infrastructure and limit the impact of landslides are: drainage devices (slope drainage, vertical drains and horizontal drains) [3], reinforcement construction (nailing and retaining: by retaining walls) and earthworks (by arranging buttresses).

New information and communication technologies have important applications in the

field of geotechnics [4] [5]. These technologies can be used, for example, for risk assessment in the geotechnical field [6]. Monitoring early detection of slope movements and landslides are essential to ensure the safety and longevity of large infrastructure projects such as the Taza-Al Hoceima expressway [1] [7]. Traditional ground monitoring techniques, although accurate, are often limited in their spatial coverage and data acquisition frequency.

In recent years, satellite remote sensing techniques, particularly Interferometric Synthetic Aperture Radar (InSAR), have emerged as innovative and powerful tools for detecting and monitoring large-scale slope movements, as well as assessing risks related to ground instabilities [8] [9].

Remote sensing, and more particularly radar interferometry (InSAR), has emerged as a powerful tool for monitoring and analyzing slope movements and landslides [9]. This technology offers several advantages over traditional monitoring methods. First, it provides significant precision, as it allows measuring ground displacements with millimeter accuracy, enabling the detection of very subtle movements that may go unnoticed during ground observations [10]. Then, it allows for wide spatial coverage, as radar images cover vast areas, allowing monitoring of entire regions and identifying high-risk areas [8]. Finally, it allows continuous monitoring, as radar satellites can acquire data at regular intervals, allowing to follow the evolution of slope movements and detect ground movements that occur between ground observations [9].

InSAR technology has revolutionized our ability to detect and monitor ground deformations over large areas with millimeter precision. Recent advances in satellite technology, such as the launch of the Sentinel-1 constellation, have further improved the temporal and spatial resolution of InSAR data [11]. The application of multi-temporal InSAR techniques (MT-InSAR), including Persistent Scatterer Interferometry (PSI) and Small Baseline Subset (SBAS), has significantly improved our ability to detect slow landslides and slope movements and assess their evolution over time [12].

The province of Taza is characterized by complex geology, combined with environmental and anthropogenic conditions favoring ground instabilities in this area in general, and along the new expressway in particular. These instabilities have a significant impact over a vast area and constitute a major threat to road infrastructure, particularly the Taza-El Hoceima expressway and its associated infrastructure. Detecting, monitoring and measuring these instabilities and land movements remains a problem, especially when dealing with very large surfaces, hence the importance of our study which addresses this problem.

The main objectives of our study are as follows: first, to detect, confirm, monitor, and measure slope movements in the Taza province, particularly along the Taza-El Hoceima expressway; second, to analyze the causative factors of these instabilities by examining the geological, morphological, and hydraulic context of the region; and finally, to identify high-risk instability zones that require long-term monitoring.

To identify and measure these instabilities and assess their risks, we will use spatial remote sensing, specifically the InSAR (Differential Radar Interferometry) technique applied to Sentinel-1 radar images, combined with spatial analysis using GIS tools. We will also analyze the main causative factors of these instabilities through a principal component analysis, which can also be applied to this type of geotechnical problems [13].

This study aims to contribute to the growing body of knowledge on the application of InSAR to landslide risk assessment on complex terrain. By focusing on a critical infrastructure project in Morocco, we hope to demonstrate the practical value of these techniques for risk management and decision-making in similar geological contexts worldwide. Additionally, our results will provide valuable information on landslide dynamics in the Taza region, supporting future sustainable infrastructure development and risk mitigation efforts.

2. STUDY AREA

2.1. Localization of the study area

The Taza-Al Hoceima expressway project aimed to develop the northern regions of Morocco with modern and improved infrastructure. It involved doubling the National Road 2 (98 km) and Regional Road 505 (50.5 km) for a total of 148.5 km, including 40 bridges and a viaduct. The

objectives of this project were to improve the level of service and qualification of the Taza-Alhoceima axis through a connection with the highway network. This project reduces the travel time between Taza and Al Hoceima from 3 to 2 hours, and has improved road safety.

Due to various geotechnical challenges, the cost of the project increased from 2.5 to 3.3 billion Dirhams, notably because of problems in the earthworks phase.

Our study focuses on a 98-kilometer linear section of this expressway, as well as the area of Taza province which contains this section subdivided into four distinct Lots as presented in Figure 1.

- Lot 1 extends over a linear distance of 6 kilometers, starting from the intersection connecting RN29 and RN6 to the interchange towards highway A2.
- Lot 2, going from PK6+000 to PK35+000, crossing the city of Jebarana.
- In Lot 3, the road extends from PK35+000 to PK62+000, offering an exit to Aknoul.
- Finally, Lot 4 connects PK62+000 and PK98+000, crossing the city of Kasseta.

Figure 1: The linear of the Taza-Al Hoceima expressway subject of our study

2.2. Mapping the characteristics of the study area

In the following part, we will present all the maps, that we created using GIS tools (ArcGIS, Global Mapper), concerning the geographical, topographical, geological, structural, meteorological and hydrological framework of the study area.

2.2.1. Geographical and topographical framework

The province of Taza is characterized by a varied and picturesque topography. The reliefs are diverse, ranging from verdant valleys to imposing mountains. Figure 2 shows that altitudes fluctuate considerably, with peaks reaching up to 1907 meters. Below, the plains extend to minimum altitudes of 258 meters.

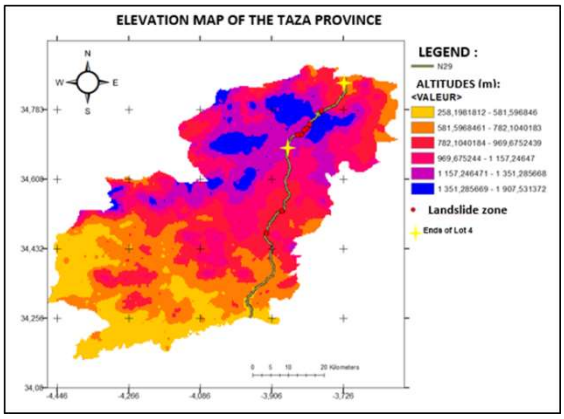

Figure 2: Elevation map of the province of Taza

Figure 3 shows that the slopes along the expressway display slopes varying from 15 to 65 degrees.

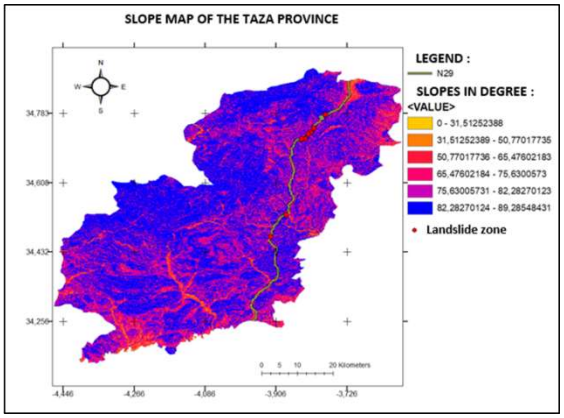

Figure 3: Slope map of the province of Taza

According to Figures 2 and 3, Lot 4 of the expressway faces significant challenges, mainly due to land movements and especially landslides. This section is particularly characterized by rugged topography and steep slopes along the slopes bordering the road. These topographical conditions make this area more vulnerable to ground instabilities, thus exacerbating the risks to the stability of the road infrastructure.

2.2.2. Geological and lithological framework

Journal of Theoretical and Applied Information Technology
15th December 2024. Vol.102. No. 23

ISSN: 1992-8645 www.jatit.org E-ISSN: 1817-3195

The study area is located in the central Rif in general, a geologically diverse region, characterized by the presence of marls, limestones and clays. This area is divided into three main units: the Intra Rif (Tangier-Ketama), the Mesorif and the Pre-Rif. The sedimentary rocks of this region have a variable limestone content: from 100 to 95% for limestones, from 65 to 35% for marls, and from 5 to 0% for clays [14]. The geological characteristics indicate low cohesion and sensitive internal resistance of the central Rif, thus reflecting the structural fragility of the region. The province of Taza is located in the particular domain of the Subrif structure, which is a transition zone between the Mesorif and the Pre-Rif [15]. The geological formations of the Pre-Rif and Mesorif can overlap in this area due to tectonic movements, thus creating a complex mosaic of rocks of different origins and ages. The Subrif suggests the presence of folds and faults in the area. These geological structures play a major role in the distribution of Jurassic outcrops and influence the geometry of rock formations.

The presence of flysch nappes testifies to the sedimentation of fine materials in this region. Moreover, the high density of faults in this area as indicated in Figure 4 below, underlines the intense tectonic activity that has shaped the local geological landscape. These faults may have played a crucial role in the distribution of sediments and rocks in the region, as well as in the genesis of the reliefs and geomorphological features observed in the Subrif.

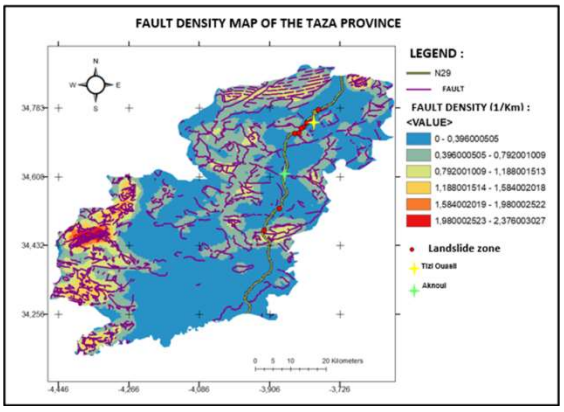

Figure 4: Fault density map of the province of Taza

Based on the lithology mapped in Figure 5 below, along the expressway, different geological formations are observed in the different lots. In Lot 4, we mainly find alluvium, marly limestones (C3-6) and detrital limestones (e2-5 AK). These formations are characterized by their varied composition, with mixtures of detrital and calcareous materials, which generally confers low cohesion and relatively low resistance. In Lot 3, the lithology is dominated by the presence of marly limestones and limestones (C1-2), indicating a similar composition but with a different distribution of geological components compared to Lot 4. As for Lot 2, we mainly observe light marly limestones (m4), sandstones and conglomerates at the base of the formation (m1-3). These types of soils also have low cohesion and low internal resistance, making them subject to movements and instabilities, especially in the presence of loads or external stresses such as climatic variations or construction activities.

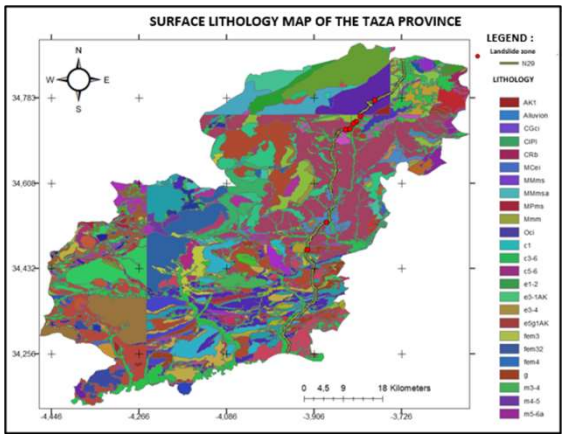

Figure 5: Lithological map of the province of Taza

In summary, the lithological diversity along the expressway reflects a variability in the composition of soils and rocks, directly influencing their mechanical behavior and susceptibility to movements and instabilities. Adequate consideration of these geological characteristics is essential when designing and constructing infrastructure in the region.

2.2.3. Meteorological and hydraulic framework

The province of Taza experiences variable rainfall depending on the areas, but generally humid. According to Figure 6 below, which presents the annual rainfall data from the Directorate-General for Hydraulics (1990-2020), precipitation ranges between 600 and 800 mm in the areas crossed by the Taza-El Hoceima expressway. This information is essential for assessing landslide risks and taking preventive measures to protect this road infrastructure.

Journal of Theoretical and Applied Information Technology
15th December 2024. Vol.102. No. 23

ISSN: 1992-8645 www.jatit.org E-ISSN: 1817-3195

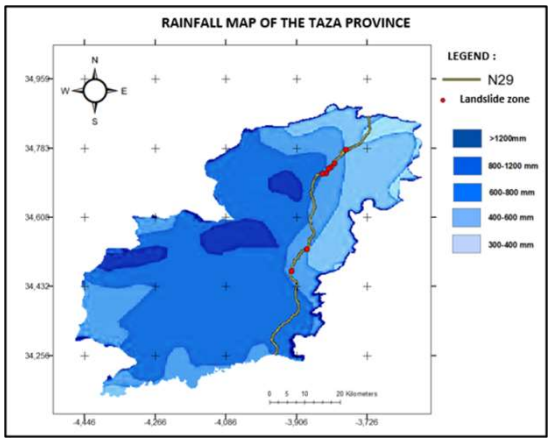

Figure 6. Rainfall map (General Directorate of Hydraulics 1990-2020)

The types of soils encountered in the region are vulnerable to erosion and alteration during periods of precipitation, which leads to a decrease in silica content (SiO2), a chemical composition that attributes the resistance character of different rock types. We can also cite the example of pelite which becomes pasty, thus favouring mudflow-type landslides. Marls are also subject to a swelling phenomenon when they absorb water and shrinkage during dry periods. Swollen marls become more susceptible to deformation and displacement, which promotes creep-type landslides in case of soil overload. In combination with accentuated slope and topography criteria, the probability of triggering land movements increases.

The province of Taza presents a remarkable geographical and hydrological diversity. Indeed, focusing on the expressway connecting Taza to Al Hoceima, it is essential to note that the drainage density in this road varies between 77 and 161 km/km² as indicated in Figure 7. This range of density reflects a significant range of water flows that can influence the stability and durability of this road infrastructure.

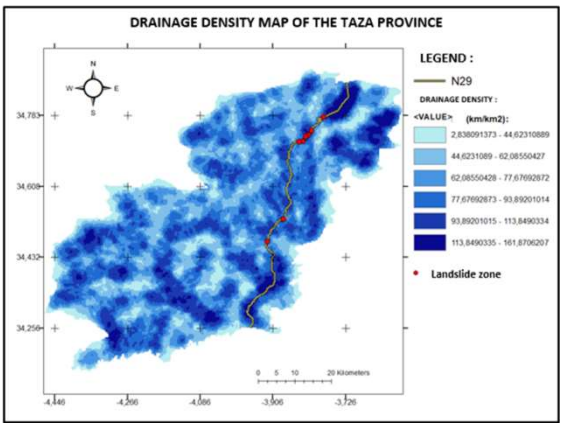

Figure 7. Drainage density map of the province of Taza

With such diverse values, surface water management becomes of paramount importance to ensure the safety and functionality of the road. Effective drainage strategies, such as the construction of appropriate drainage channels, and the implementation of storm water management techniques, are necessary to prevent flooding, reduce soil erosion and alteration, and maintain the integrity of the expressway.

3. MATERIALS AND METHOD

3.1. Methodological approach

The approach of our study is based on technique (InSAR) that allows measuring ground displacements by comparing the phases of radar waves acquired at different times [16]. The basic principle of InSAR is that the radar wave reflected by an object on the earth's surface undergoes a phase shift if the object moves between the two acquisitions. This phase shift is proportional to the displacement of the object, and can be measured with great precision [17] [18].

Certain elements such as phase, intensity and coherence are fundamental in the analysis and interpretation of radar images, providing detailed information on the Earth's surface and its changes over time. The phase (Φ) represents the angle of the reflected radar wave, indicating the relative distance between the satellite and the Earth's surface. It is essential for determining terrain variations and displacements of the earth's surface. The intensity (I) measures the amplitude of the radar signal reflected by the earth's surface. The coherence (γ) quantifies the similarity of phase and amplitude between two radar images acquired at different times or angles. It is used to evaluate the

quality of radar interferometry (InSAR) and detect changes in the earth's surface [17] [18]..

The interferometric phase is a combination of several factors that must be corrected. This phase is the contribution to displacement that comes from the result of subsidence or uplift, however there are a number of other terms that must be subtracted such as the flat earth phase which is the result of the earth's curvature, the topographic contribution, the atmospheric contribution which is the result of the difference of several parameters such as humidity, temperature and pressure between the two SAR acquisitions [16] [19]. Finally, there is also noise that is introduced in the phase change due to temporal changes for example between scatterers or different look angles between the two acquisitions [20]. The basic equation of InSAR is presented in Figure 8 [17].

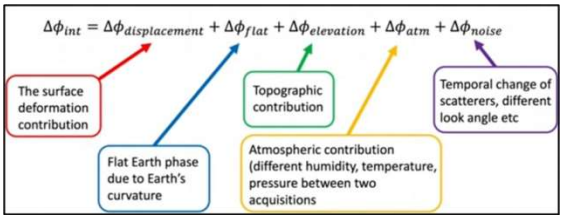

Figure 8: Factors of the interferometric phase

Despite its advantages, the application of InSAR on complex area like the province of Taza presents several challenges. These include geometric distortions in SAR imagery due to steep topography, temporal decorrelation in vegetated areas, and atmospheric interference [21]. However, recent studies have demonstrated the potential of advanced InSAR techniques to overcome these limitations and provide valuable information on landslide dynamics, even in challenging environments [22].

The InSAR process includes several steps, the main ones being: Data acquisition, Preprocessing (to eliminate noise and errors and prepare data for analysis, Co-registration (to align the radar images correctly), Interferogram formation (by subtracting the phase of one image from the phase of the other image), Phase unwrapping (to obtain actual displacements in meters). Topographic correction (to obtain actual displacements due to ground movements) and Displacement analysis (to identify high-risk landslide areas and to understand the causes of movements).

3.2. The steps followed in carrying out the study

To carry out our study, we followed a methodology with four steps.

The first step consisted of exploring the region, acquiring and collecting data to:

- Map geological, topographical, and environmental data. These data were presented in the study area section.
- Identify factors responsible for ground instabilities.
- Create a database for geotechnical evaluations and analyses of our study.

Then, the second step concerned the location, confirmation and measurement of landslides along the expressway, through:

- Locate and monitor landslides triggered along the Taza-El Hoceima expressway during the period of construction works of this road, using the GIS tool and information collected in the field
- Initiate spatial analysis through optical satellite images.
- Strengthen the confidence and reliability of the results of the SNAP S-1 software, by confirming this location through InSAR.
- Proceed to the measurement of the vertical displacements of the detected landslide areas

The third stage involved statistical analysis, using principal component analysis (PCA) to identify the predominant causal factors of the landslides identified initially. An analysis of the environmental characteristics of these areas made it possible to confirm the causative factors.

In the fourth and final step, we determined the movement sites constituting high-risk zones within our study area using InSAR and displacement maps. We measured the displacements in these zones and attempted to explain them by analysing their lithological, topographical, geological, meteorological, and other characteristics.

3.3. Collected data

Radar satellites use different frequency bands to acquire images: C-band, X-band, L-band and others. Each band is adapted to a specific application. C-band (wavelength of about 6 cm): It is widely used due to its ability to penetrate through clouds and rain, making it ideal for monitoring ground movements [10] [19].

We opted for the use of the Sentinel-1 satellite which is an active satellite, it works with the C-band, whose wavelength is approximately 6 cm. The choice of the S1 satellite is due to the continuous accessibility of its high-quality radar data since 2014, unlike other SAR satellites whose data access is limited or whose operation ceased before this date. Figure 9 specifies the acquisition parameters of the S-1 radar products used in the InSAR method.

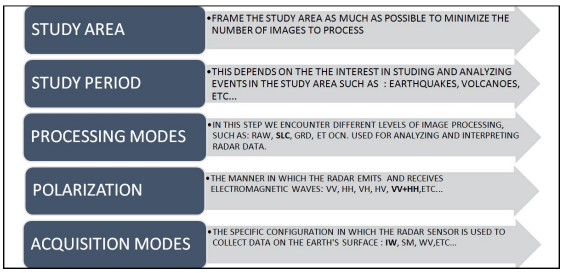

Figure 9. Schematization of the acquisition parameters of SAR products

The images acquired for our work by the Sentinel 1A satellite date from March 15, 2015, June 1, 2016, October 13, 2018 and April 5, 2020. The acquisition sources of our products are the platforms: ASF Data Search and Copernicus Browser. The acquisition of images was done by choosing the appropriate options and respecting the essential steps [23].

For the analysis of our project, we used the SLC (Single Look Complex) processing mode, which offers superior spatial resolution and image quality, essential for accurate detection of displacements and terrain variations.

For polarization, we chose the VV+HH configuration, which combines vertical and horizontal components, and allows for better sensitivity to different characteristics (textures and structures) related to the ground.

We opted for the IW (Interferometric Wide) mode, which is used to obtain wide spatial coverage and high spatial resolution. The IW acquisition mode is particularly suitable for monitoring vast areas, making this method ideal for our study of ground instabilities along the Taza-El Hoceima expressway. During acquisition for the IW mode, each pixel of the image represents an area of 5 m by 20 m on the ground, over an extent of 250 km [24].

3.4. Materials

To carry out our study, we used Sentinel-1 radar image data, as well as the SNAP (Sentinel Application Platform) software to perform InSAR analyses. In addition, we used Google Earth Pro software to identify and confirm land movements, as well as GIS tools to map these land movements and the characteristics of the study area. Finally, we used IBM SPSS software to perform Principal Component Analysis (PCA) to determine causative factors. The SNAP software is a platform developed by ESA (European Space Agency) that offers a complete suite of open-source tools for processing, visualizing and analyzing satellite data.

Figure 10 below schematizes the process of measuring vertical displacements performed by SNAP [24].

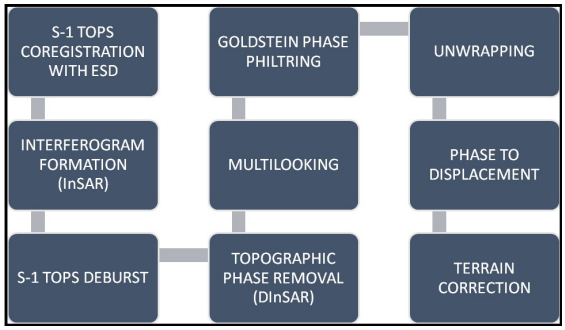

Figure 10. Schematization of the vertical displacement measurement process by SNAP

Google Earth Pro software: it allows us to locate ground movements and identify high-risk areas. It allows visualization of optical images of the Earth's surface. It allows identification of landslide areas and thus helps in measuring vertical displacements.

GIS tools (ArcGIS, Global Mapper): to map the geological context and causative factors of landslides. They thus allowed mapping of geological formations, faults, slopes, drainage densities as well as precipitation.

Principal Component Analysis (PCA) by IBM SPSS allowed identification of the predominant causative factors of landslides. Indeed, the data analysis was able to first identify the variables that contribute most to landslides. Then it allowed the creation of new variables (principal components) that are uncorrelated.

4. RESULTS AND DISCUSSION

4.1. Evaluation Of Land Movements Along The Expressway: Identification And Confirmation

4.1.1. Identification of land movements along the expressway

We initially chose to identify land movements using information and data from the field, which correspond to the period of the study, and Google Earth due to the clarity of the images and the temporal history option, which facilitates the identification of slope movements and landslides along the road during the construction period. This method constitutes a reliable reference and a real database, serving as a foundation for our analyses. Based on this data, we can then use the InSAR technique to confirm these land movements and strengthen the reliability of our interpretations of the results obtained by InSAR. Figure 11 below shows the slope movements zones identified along the Taza-El Hoceima expressway.

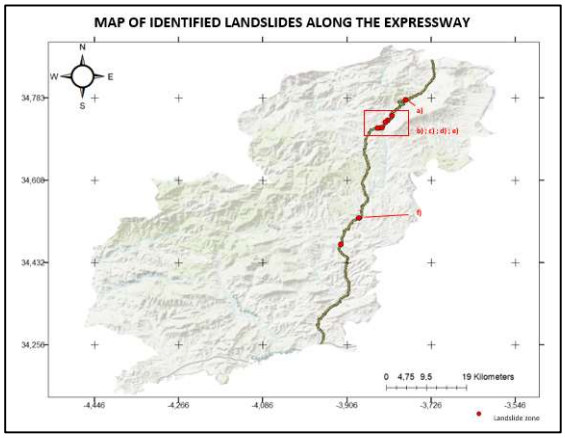

Figure 11: a) b) c) d) e) f): slope movements zones triggered along the Taza-El Hoceima expressway

4.1.2. Confirmation of identification by InSAR through image intensity difference

The intensity difference between two images acquired on two different dates at the same location can show the existence of anomalies, or a formation that was present in the first image (Master image) and was absent in the second image (secondary image), or it can show that this formation has been modified; the opposite is also true.

The intensity difference of landslide site a), previously identified, between the master image acquired on June 11, 2016, and the image of October 13, 2018, is clearly shown in Figure 12.

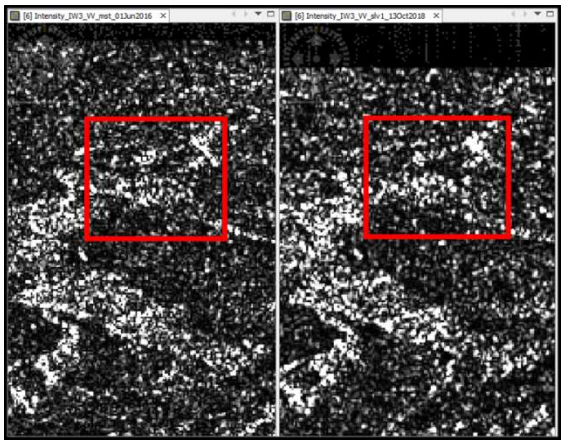

Figure 12: Confirmation of the identification of landslide site a) by intensity difference

4.1.3. Confirmation of identification by InSAR through RGB composition of images

For better visualization in the SNAP software, we superimpose the two intensities in an RGB colored image. The intensity of the master image is colored in red and in green for the secondary image. The figure 13 must be interpreted as follows:

- Yellow colored areas mean that the same formation is found in both images, nothing has changed.
- Red areas mean that the formation is present in the first image, but absent in the secondary image.
- For green areas, the formation present in the secondary image was not previously present in the first.

Figure 13 below confirms in RGB composition the landslide of site c) previously identified. Knowing that normally to confirm the landslide of site c), its location in the RGB composition should be colored green, or the green pixels should dominate.

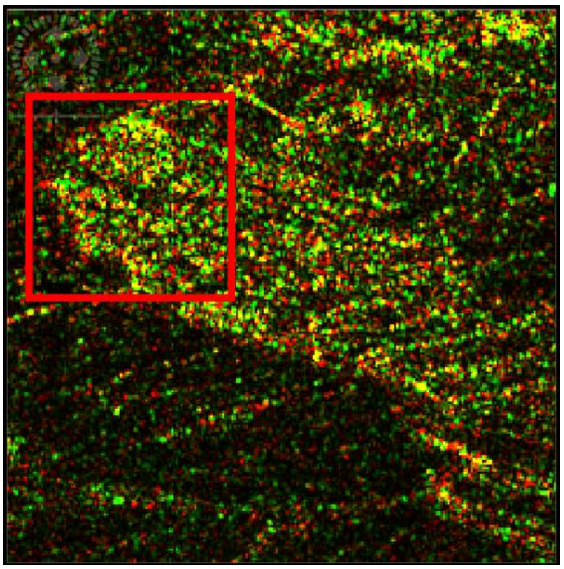

Figure 13: landslide site c) 2016-2018, confirmed by RGB composition of images

4.1.4. Confirmation of this identification by InSAR through phase and coherence difference

The visualization and detection of landslides do not stop at the intensity and RGB composition of images. Indeed, the analysis of phase and coherence difference also allows identifying anomaly sites. Figure 14 represents the phase difference between the three study dates.

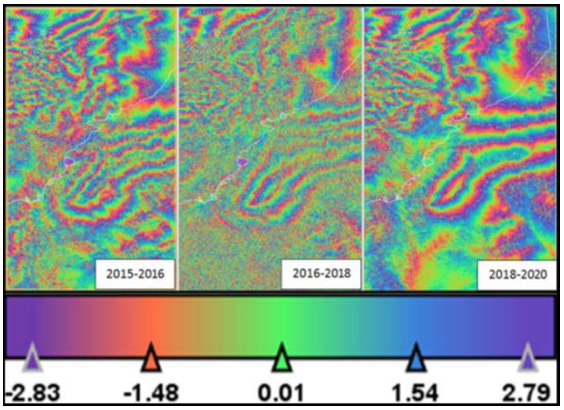

Figure 14: Phase difference for the three study periods

The analysis of the phase map during the study periods detects anomalies of ground movements in the (X, Y) plane. Areas with very light-colored circles correspond to accentuated altitudes and morphologies, in the form of mountains and valleys. Areas with very tight circles present the transition phase towards sites that record anomalies. We can therefore locate these anomalies by observing phase discontinuities outside and at the extremity of these areas of very tight circles.

The previously identified landslides are also located in phase discontinuity locations as shown by the polygons projected in the phase maps above (Figure 14). The white line projected in this figure represents the expressway.

For areas presenting phase noise without distinct phase circles, this may be due to the effect of topography that is not perfectly corrected or to weather conditions.

The passage of lines that cut and deform the circles in Figure 15 cannot always indicate fault activity. It may also be a ground movement anomaly due to other factors, or it may be a flow line. It is possible that water is not present, but that it is a water path, which is evidence. It is therefore possible to delineate watersheds using phase maps.

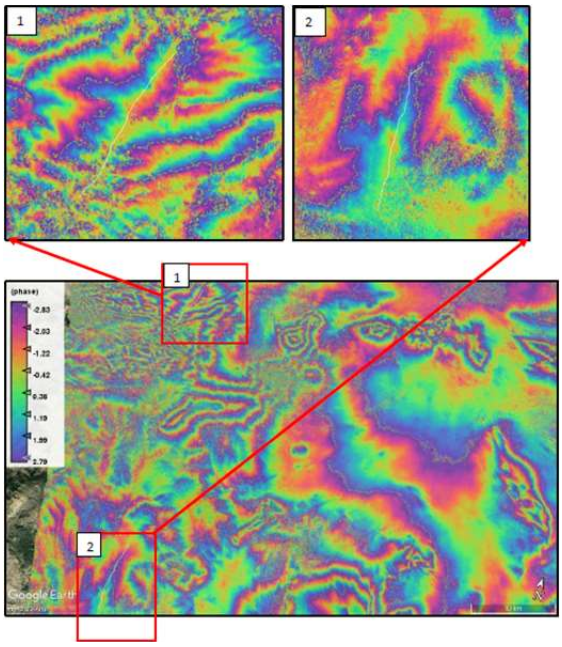

Figure 15: Phase map (2018-2020)

To demonstrate that these are flow lines, the coherence map reinforces this argument, we filtered a coherence map whose value is less than or equal to 0.3, represented in Figure 16.

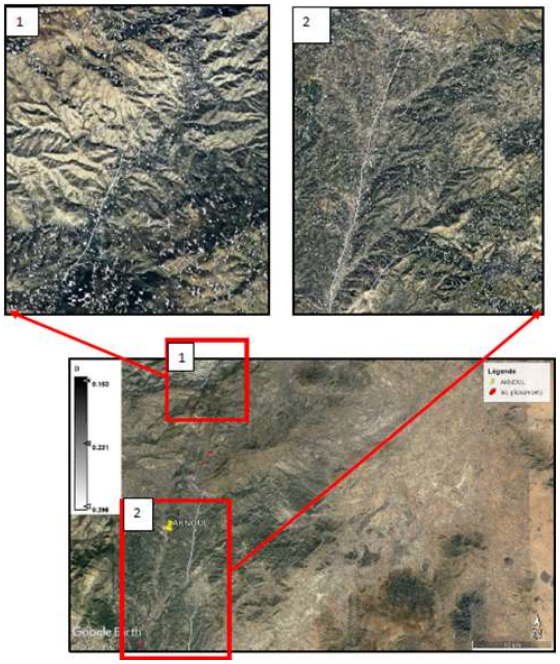

Figure 16: Coherence map (2016-2018) whose value is less than or equal to 0.3

The coherence of landslide areas identified by phase maps and RGB composition maps is obviously low, and varies between 0.34 and 0.53, as it is identified by the polygons in Figure 17.

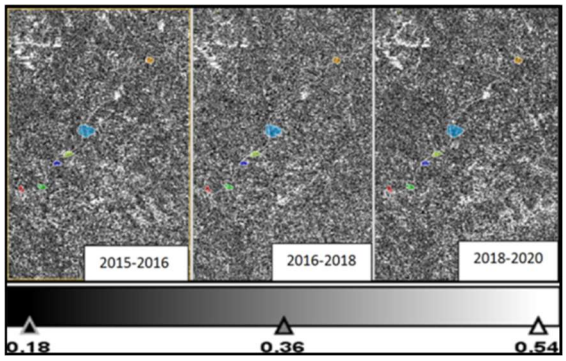

Figure 17: Coherence maps

Therefore, low coherence areas detect anomalies as well as water basins, lakes or others.

4.2. Vertical Displacement Measurement By InSAR

4.2.1. Confirmation of identification by InSAR through vertical displacement measurement

Vertical displacement measurement also requires the InSAR technique. Indeed, by using the SNAP S-1 software, the SNAPHU bibliography (Statistical-Cost Network-Flow Algorithm for Phase Unwrapping), and GIS tools (Google Earth Pro, ArcGIS, Global Mapper), we succeeded in extracting the vertical displacement results and mapping them in the study area for the different study periods indicated in Figures 18, 19 and 20. Figure 18 presents the vertical ground displacements in the period between 2015 and 2016.

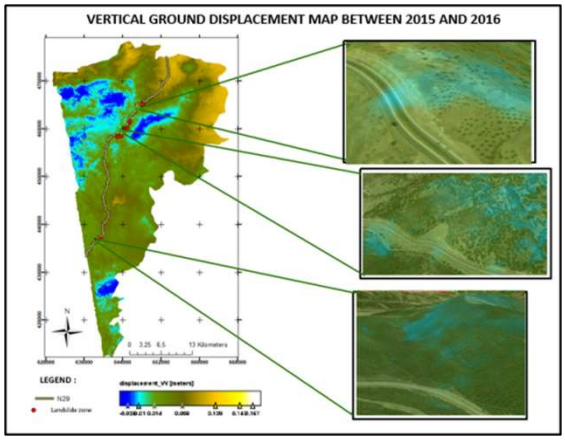

Figure 18: Vertical ground displacement map between 2015 and 2016.

Figure 19 presents the vertical ground displacements in the period between 2016 and 2018.

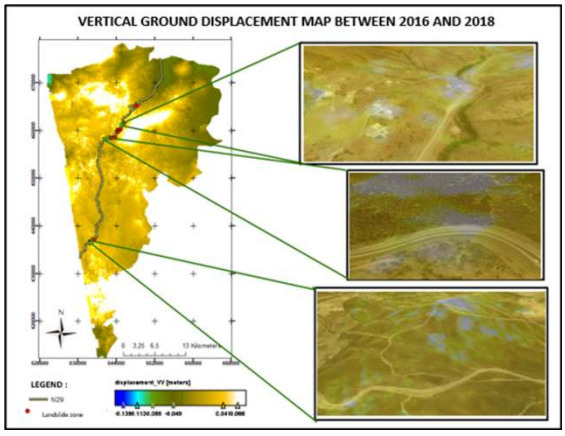

Figure 19: Vertical ground displacement map between 2016 and 2018.

Figure 20 presents the vertical ground displacements in the period between 2018 and 2020.

Journal of Theoretical and Applied Information Technology
15th December 2024. Vol.102. No. 23

ISSN: 1992-8645 www.jatit.org E-ISSN: 1817-3195

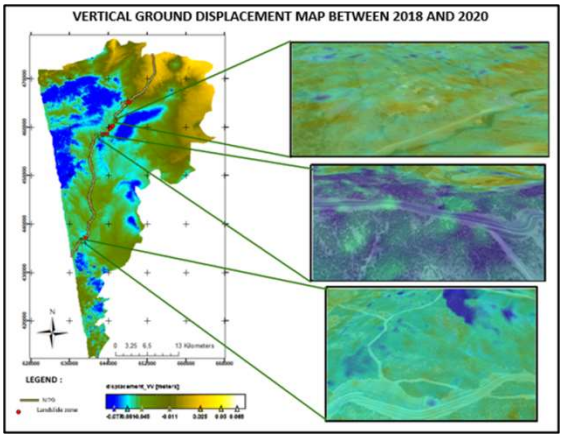

Figure 20: Vertical ground displacement map between 2018 and 2020.

The images indicated in the displacement maps identify previously identified landslide sites along the expressway, which record significant displacements during the three study periods.

The extraction and mapping of vertical displacement results in the study area for the indicated periods, coupled with field information concerning landslides triggered during the expressway construction period, allowed us to confirm the six landslide sites along the expressway. These sites recorded significant displacements during the three study periods. Next, we will present the results of vertical displacement measurements of the identified sites.

4.2.2. Result of the vertical displacement measurement

To quantify and explain the deformations, we projected the identified sites along the expressway by drawing polygons on the vertical displacement maps (Figures 18, 19, and 20) to provide average displacement values for each landslide site, and also to understand the contributing factors to the landslides triggered during the expressway construction period (our study period).

The results of this approach provided the average displacement values within the landslide polygons, as presented in Table 1.

Table 1: Average displacements of identified landslide polygons

Polygon	Area (Hectare)	Displacement (cm) 2015-2016	Displacement (cm) 2016-2018	Displacement (cm) 2018-2020
a)	9.11	-4	2.59	-6.1
b)	33.9	-6	5.7	-5
c)	8.1	-5	5.95	-3
d)	6.53	-5	4.35	-3.4
e)	7.44	-7	3	-3.3
f)	22.2	-6.37	5.1	-2.9

In the following results, we will determine the causes of the significant displacements recorded through a PCA analysis, and we will attempt to confirm these results by analyzing the characteristics of the identified areas.

4.3. Determination and confirmation Of Causative Factors Of Identified Land movements

4.3.1. Determination of Causative Factors Of Identified Land movements By PCA Analysis

Principal Component Analysis (PCA) is a quantitative approach that serves both to analyze and reduce the variables of causative factors of the landslides identified above. This method transforms these variables into a new set of uncorrelated variables, this set is called a principal component or a factorial axis.

The first component is formed by the maximum number of possible variables, the second component is formed by fewer variables than the first, and so on. The variable that correlates well with a factorial axis means that this variable has a strong contribution to the formation of this axis, in other words, the variable has a strong projection on the vector.

Using IBM SPSS Statistics software, we performed principal component analysis, based on data collected from cartographic maps. Table 2 summarizes the input data for the analysis (PCA).

Table 2: Input data for PCA analysis

Figure	Height	Slope	Fault	Cohesion	Precipitation	Drainage
a	591.00	38.40	20	12.00	500.00	103.87
b	429.00	35.20	20	30.00	700.00	137.00
C	653.00	39.70	59	30.00	700.00	137.00
d	443.00	28.90	59	35.00	700.00	137.00
e	483.00	41.90	59	45.00	1000.00	85.78
f	643.00	21.00	20	40.00	700.00	85.78

Name	Type	Width	Label
Figure	Chain	8	
Height	Numeric	8	Height of slopes (m)
Slope	Numeric	8	Slope of terrain (%)
Fault	Numeric	8	Density of faults (1/km)
Cohesion	Numeric	8	Soil cohesion (Kpa)
Friction Angle	Numeric	8	Angle of friction (°)
Precipitation	Numeric	8	Annual precipitation (mm)
Drainage	Numeric	8	Drainage density (km/km²)

The result of the principal component analysis gives the component matrix, represented in Table 3 below.

Table 3: Component matrix

Component Matrix *

	Components		
	1	2	3
Height of slopes (m)	-,415	-,154	-,470
Slope (%)	,234	-,775	,556
Density of faults (1/km)	,721	,035	,395
Soil cohesion (Kpa)	,849	,357	-,368
Friction angle (*)	-,047	,985	,087
Annual precipitation (mm)	,971	-,095	-,152
Drainage density (km/km²)	-,167	,436	,863

According to the matrix above:

- Variables that are well correlated with axis 1: fault density, soil cohesion, and rainfall.
- Variables that are well correlated with axis 2: slope of embankments, and friction angle.
- Variables that are well correlated with axis 3: slope of slopes, and drainage density.

After reducing the number of axes by calculating the variance of components, we find:

- Component 1 presents 34.9% of the formation
- Component 2 presents 27.5% of the formation

A cumulative 62.4% of formation is significant, therefore we take axis 1 and 2 for the rest of this analysis.

Then we need to give meaning to each axis for the plot presented in Figure 21, in order to reduce the variables of causative factors of previously identified landslides.

For axis 1: if the landslide is close to this axis in the positive part, the causative factors are therefore soil cohesion and rainfall in the first place, as well as fault density. In the negative part of this axis, the variable that plays in the landslide is the height of slopes.

For axis 2: in the positive part of this axis, the causative factors are therefore the friction angle in the first place, as well as drainage density. In the negative part of this axis, the variable that plays in the landslide is the slope.

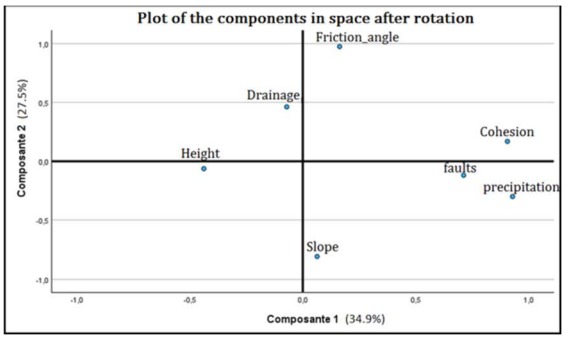

Figure 21: Plot of principal components in the plane (comp1, comp2)

By adopting just two principal components, since as mentioned a percentage of 62.4% of information is sufficient in our analysis to reduce the dimensions of variables. We therefore find the distribution of identified landslides in the plane represented in Figure 22 below.

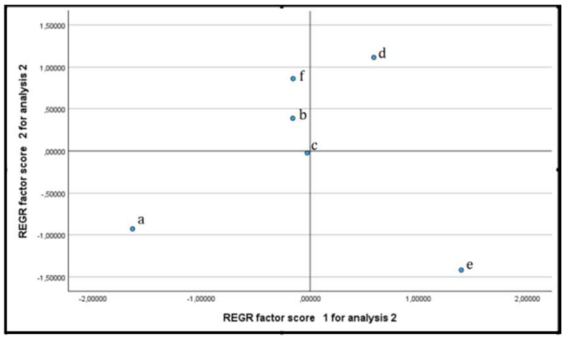

Figure 22. Distribution of identified landslides in the plane (comp1, comp2)

According to the distribution of identified landslides, in the plane above (figure 22), we can reduce the variables of causative factors of landslides in table 4 below.

Table 4. Determination of causative factors of identified landslides

Landslide zone	Factors of Lanslides
a)	• Height of slope (-0,4)* • Slope (-0,8)
b)	• Friction angle (0,9) • Drainage density (0,46)
c)	Point c is poorly represented
d)	• Friction angle (0,9) • Drainage density (0,46)
e)	• Annual Precipitation (0,93) • Soil cohesion (0,91) • Density of faults (0,7)
f)	• Friction angle (0,9) • Drainage density (0,46)

The mentioned values indicate the eigenvalue of the projection of the factor in the axis that correlates well with this variable. Some of these factors have been confirmed by other recent studies as the main causes of landslides in the northern region of Morocco, using other methods like machine learning approach or GIS [25] [26].

4.3.2. Confirmation and explanation of causative factors of identified Landslides along the road infrastructure

To better understand the causative factors of these landslides, we analyzed the characteristics of the sites: lithology, rainfall, faults, and drainage. Indeed, the data collected from the maps produced for the study area and the displacement maps help highlight the various geotechnical processes responsible for subsidence and uplift in the identified landslide zones. Table 5 below presents the lithology of the six sites.

Table 5: Summary of the lithology of the identified landslides

Landslide zone	Lithology
a)	Red salt clay
b)	Dark pelite with limestone intercalations
c)	Dark pelite with limestone levels crossed by alluvium
d)	Dark pelite intersected with limestone and marl-limestone levels
e)	Dark pelite with limestone levels
f)	Dark pelite with limestone levels

First, the subsidence recorded in these landslide areas can be mainly attributed to soil consolidation, particularly in zones characterized by clay formations such as zone (a). The red saline clays present in this area undergo a progressive consolidation process, resulting in slow subsidence over time. Additionally, the dissolution of soluble rocks such as limestone, present in varying quantities in all formations of these zones, also contributes to the formation of cavities and sinkholes, thereby increasing the likelihood of settlements due to soil decompression or overload resulting from vibrations of the construction works. The amount of salt in zone (a) further increases the probability of solubility in this area. Excessive pumping for irrigation or drinking water supply can also lead to a decrease in the groundwater level, causing soil compression.

Moreover, the uplifts observed on the displacement maps between 2016 and 2018 are primarily due to soil swelling, such as pelite, a type of soil present in most of these landslide areas. This swelling is generally caused by soil water saturation, particularly in zones with high drainage capacity like site (c), characterized by the presence of alluvium facilitating water flow and infiltration. Additionally, the rise in groundwater levels during significant rainfall periods, freeze-thaw cycles during cold periods, and temperature variations causing thermal expansion of soils and rocks also contribute to the recorded uplifts. Natural geological processes, including tectonic movements, can sometimes cause uplifts. This region is characterized by high seismicity and frequently experiences earthquakes felt by the inhabitants. Consequently, tectonic movements are constant and play a significant role in the activation of pre-existing faults. Among the most affected zones by a high density of faults are zones (c), (d), and (e).

We then attempted to explain certain significant displacements recorded during the study periods by analyzing the rainfall characteristics and the faults in the studied area. Figure 23 shows an overlay of the characteristic maps.

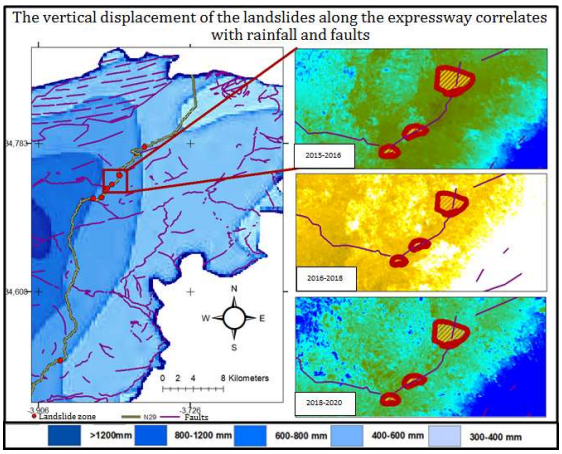

Figure 23: Correlation between rainfall, faults and displacements

Figure 23 shows that the significant displacements recorded during the study periods clearly correspond to areas with high precipitation and the presence of a continuous fault system linking three previously identified landslides (b, c, and d).

Finally, we attempted to explain the displacements based on drainage density. Figure 24, which presents the overlay map of drainage density and faults, clearly shows that the high values indicated on the displacement maps correspond to areas with high drainage density.

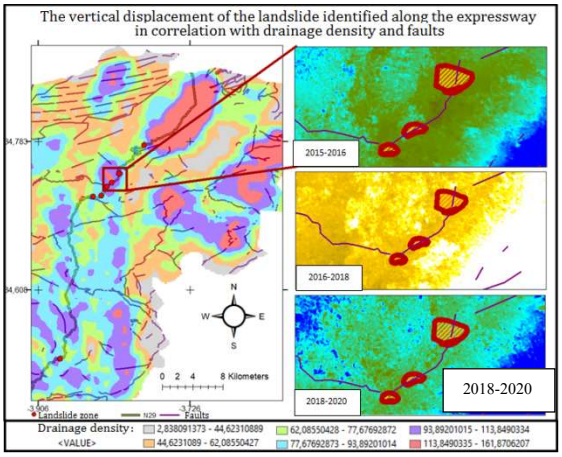

Figure 24: Correlation between displacement and drainage density

Using InSAR, we were able to extract vertical displacements with millimetric accuracy. We also explained these displacement results using data on precipitation, faults, drainage density, and the characteristics of the region's malleable, clayey, and swelling soils. These conditions facilitated the landslides identified and confirmed by InSAR and field data. In the subsequent results, we will use InSAR to identify high-risk areas of terrain instability.

4.4. Identification and Explanation of High-Risk Zones in the Study Area

4.4.1. Identification of high-risk zones using displacement maps

The assessment of risks associated with terrain instabilities can be approached using two distinct methods: qualitative and quantitative [27]. Qualitative methods involve field visits, map analysis, and instability inventories to evaluate the nature and extent of risks. In contrast, quantitative approaches rely on statistical and geotechnical analyses to quantify risks with precision. In our study, we primarily focus on the first approach, emphasizing the importance of field visits, cartographic analysis, and detailed information in evaluating land instability risks.

To achieve our objective, we utilized the displacement maps presented in Figures 18, 19, and 20. Measuring vertical displacements required the use of the InSAR technique, as explained previously. Our approach also involved correlating InSAR data with field observations and other geospatial information to provide a comprehensive analysis of land movements.

While generating these maps (Figures 18, 19, and 20), we observed continuous displacements in the same areas throughout the study periods, thus confirming the landslides that occurred during the expansion works of the Taza-El Hoceima expressway and its geometric improvement.

Using the displacement maps, we identified examples of high-risk areas that exhibit extreme values on the displacement scale. Figure 25 shows the polygons of these areas projected onto the displacement maps.

Journal of Theoretical and Applied Information Technology
15th December 2024. Vol.102. No. 23

ISSN: 1992-8645 www.jatit.org E-ISSN: 1817-3195

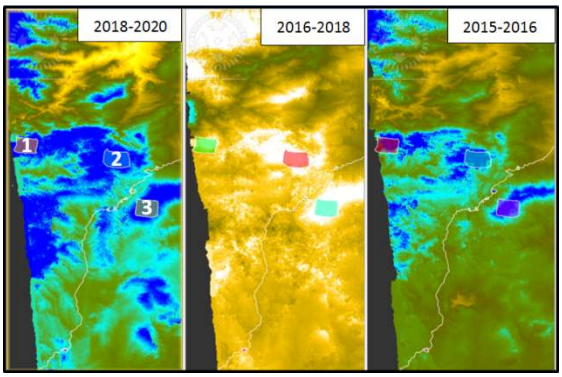

Figure 25: Projection of previously identified high-risk areas 1) Jebel Merzouk 2)Azrou Akchar 3)Jebel Berkane

The following table 6 provides the displacement values for these sites during the study periods.

Tableau 6: Average displacement of polygons in high-risk areas 1) 2) and 3)

Polygon	1. Jebel Merzouk	2. Azrou Akchar	3. Jebel Berkane
Area (Hectare)	593	556	646
Displacement (cm) 2015-2016	-3 à -7	-4.2 à -7	-2 à 4
Displacement (cm) 2016-2018	5 à 9	6 à 10	9 à 10
Displacement (cm) 2018-2020	-8 à -11.5	-9 à -14.34	-8 à -10
Average total Displacement (cm)	-7.75	-9.27	1.5

In the subsequent results, we focused on explaining the high-risk zones identified by their various lithological, geological, and topographical characteristics.

4.4.2. Discussion and explanation of high-risk zones identified by displacement maps

To seek the consistency of these results, we overlaid the displacement maps (Figures 18, 19, and 20), the lithological map (Figure 5), and the fault map (Figure 4). The result of this overlay is presented in Figure 26.

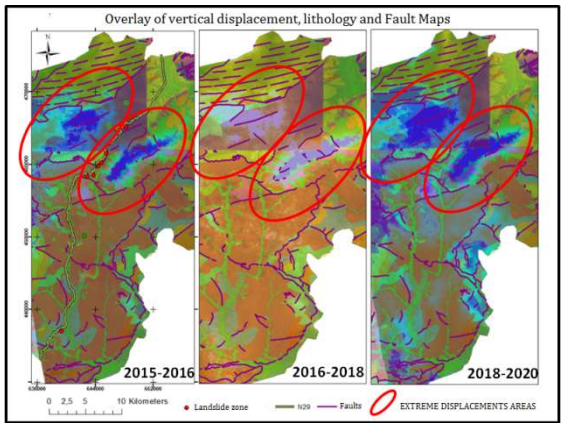

Figure 26: Overlay of vertical displacement map on lithology and fault maps

The analysis of this map shows consistency in the results. Indeed, the identified high-risk zones correspond to sites with a high density of faults, combined with specific geological formations presented in Table 7. These types of soils promote all kinds of ground movements, including vertical displacements, especially in the presence of water flow and other anthropogenic factors such as precipitation and drainage density, which justify these identified displacements.e Table 7 summarizes the lithological characteristics of these zones.

Table 7: Lithological formations of the high risk areas

High-risk areas	Lithological formations
1. Jebel Merzouk	Sandstone and pelite series
2. Azrou Akchar	Clays and red sandstone
3. Jebel Berkane	Alluvium, marl and sandstone with limestone

These high-risk zones also record significant topographic values (areas shaded in blue), and their slope degrees are also noteworthy (areas shaded in orange), as shown in Figure 27.

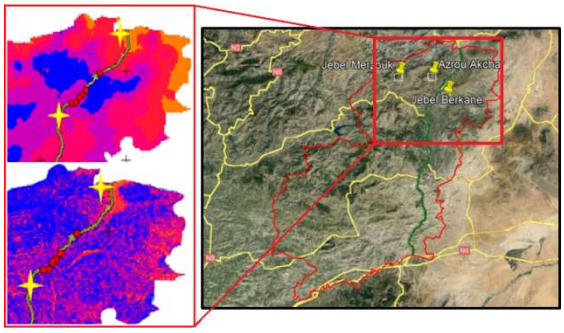

Figure 27: Capture of topography and slope maps for the three identified high-risk areas 1)Jebel Merzouk 2)Azrou Akchar 3)Jebel Berkane

These continuously moving zones, identified during our study period, could potentially pose risks to the safety of their infrastructure and inhabitants, highlighting the need to continue monitoring their evolution over time.

5. CONCLUSION AND PERSPECTIVES

The Taza-Al Hoceima expressway project represents a major investment for northern Morocco, particularly for the province of Taza. It stimulates economic development, facilitates trade exchanges, and improves access to essential services, while integrating isolated regions, thereby strengthening social cohesion and enhancing the quality of life for inhabitants.

The province of Taza, located in the Subrif region, is characterized by a complex geology with faults, folds, and strike-slip faults resulting from intense tectonic activity. The varied topography, combined with climatic conditions, soil types mainly composed of marls, pelites, and clays, as well as the high fault density, particularly in the Aknoul and Tizi Ouasli regions, creates an environment prone to ground movements and geological instabilities.

The use of remote sensing by interferometry of Sentinel-1 radar images (InSAR) via the SNAP software allowed us to detect, confirm, monitor, and evaluate ground movements, identify high-risk areas, and measure vertical displacements, thereby facilitating the monitoring of infrastructures and structures. Landslides identified using field information and Google Earth, and confirmed by InSAR, show displacements ranging from -7.51 cm to -2.05 cm during the study period. These displacements correlate well with fault density, high drainage density, and malleable soil types. Principal Component Analysis (PCA) also confirmed that these factors are the main causes of landslides. Our work also identified high-risk areas, such as the surroundings of Jebel Marzouk, Jebel Berkane, and Azou Akchar, which recorded displacements ranging from 1.5 cm to -9.27 cm during the study period. Analyzing the characteristics of these areas revealed their notable geological complexity, which is conducive to ground movements.

A prolonged study period allows tracking the evolution of landslides, while a shorter period highlights rapid movements such as flows, volcanic damage, floods, or earthquakes. InSAR, with its millimeter precision, can detect anomalies over vast areas. However, one of the main limitations of our work and method is the difficulty of perfectly visualizing landslides on small sites smaller than its resolution of 20 m x 5 m. Nonetheless, this method is excellent for monitoring large natural phenomena and detecting broader-scale anomalies.

Another possible use of InSAR is to assist in decision-making regarding routes for linear projects. Indeed, phase and coherence maps allow delineating watersheds and determining flow lines. Displacement maps thus guide decisions on route selection for linear projects. According to the spatial analyses of this project, the chosen route for the expressway was perfectly optimal. Although it crosses areas of accentuated topography, thereby increasing earthwork, it avoids zones of significant displacements, which reduces geological risks. However, this may slightly increase travel time.

Using InSAR and the collected data, and as part of the perspectives for continuing this study, it is possible to create a terrain susceptibility map. This also allows measuring displacements and monitoring subsidence or uplifts of structures and linear infrastructures, thereby ensuring their safety and durability. Additionally, we could develop a computer program that combines data from phase, coherence, and displacement maps to produce a susceptibility map. The susceptibility probability would then be more significant as the program would be conditioned to identify pixels with extreme displacement values and coherence greater than 0.3. This would exclude lakes and other water accumulation areas, whose phases are noisy and located in phase discontinuity zones, thereby increasing the reliability and efficiency of the method used.

REFERENCES:

[1] M. Zocchi, A.K. Kasaragod, A. Jenkins, C. Cook, R. Dobson, T. Oommen, D. Van Huis, B. Taylor, C. Brooks, R. Marini & al, “Multi-Sensor and Multi-Scale Remote Sensing Approach for Assessing Slope Instability along Transportation Corridors Using Satellites and Uncrewed Aircraft Systems”. *Remote Sensing*, Vol. 15, Issue. 12, no. 3016, 2023, https://doi.org/10.3390/rs15123016

[2] S. Martino, F. Bozzano, P. Caporossi, D. D’angiò, M. Della Seta, C. Esposito, A. Fantini, M. Fiorucci, L.M. Giannini, R. Iannucci & al, “Impact of landslides on transportation routes

during the 2016–2017 Central Italy seismic sequence". *Landslides*, Vol. 16, 2019, pp. 1221–1241.

[3] H. Cherifi, A. Chaouni, M. Ettayeb, I. Jabri, H. El-Asmi, I. Raini & al, "Management of rock hazard: case of the schistose excavation D8, Taza-Al Hoceima expressway, Morocco.", *Arabian Journal of Geosciences*, Vol. 15, Issue. 11, p. 1, 2022.

[4] M. Adak, A. Usmani, A. Mandal, "Integrating information technology in engineering geology: case studies and educational approaches for enhanced geological analysis for infrastructure development", *Journal of Theoretical and Applied Information Technology (JATIT)*, Vol. 102, No. 7, 2024, pp. 2968-2978.

[5] J. He, I. Barton, "Hyperspectral remote sensing for detecting geotechnical problems at Ray mine", *Engineering Geolog*, Vol. 292, 2021, pp. 2968-2978.

[6] M. Adak, A. Usmani, A. Mandal, "Enhancing large underground excavation risk assessment: optimization through information systems", *Journal of Theoretical and Applied Information Technology (JATIT)*, Vol. 102, No. 8, 2024, pp. 3423- 3433.

[7] M. Sadiki, M. Manaouch, M. Aghad, M. Batchi, J. Al Karkouri, "Identifying Landslides Prone-Areas Using GIS-based Fuzzy Analytical Hierarchy Process Model in Ziz Upper Watershed (Morocco)", *Ecological Engineering & Environmental Technology*, Vol. 24, No. 1, 2023, pp. 67-83. https://doi.org/10.12912/27197050/154916

[8] J. Wasowski & F. Bovenga, "Investigating landslides and unstable slopes with satellite Multi Temporal Interferometry: Current issues and future perspectives", *Engineering Geology*, Vol. 174, 2014, pp. 103-138.

[9] S. Mirmazloumi, Y. Wassie, L. Nava, M. Cuevas-González, M. Crosetto & O. Monserrat, "InSAR time series and LSTM model to support early warning detection tools of ground instabilities: mining site case studies". *Bulletin of Engineering Geology and the Environment,* Vol. **82**, no. 374, 2023. pp. 23. https://doi.org/10.1007/s10064-023-03388-w

[10] F. Calò, F. Ardizzone, R. Castaldo, P. Lollino, P. Tizzani, F. Guzzetti & al, "Enhanced landslide investigations through advanced DInSAR techniques: the Ivancich case study, Assisi, Italy", *Remote Sensing of Environment*, Vol. 142, 2014, pp. 69–82, https://doi.org/10.1016/j.rse.2013.11.003

[11] E. Intrieri, F. Raspini, A. Fumagalli, P. Lu, S. Del Conte, P. Farina & al, "The Maoxian landslide as seen from space: detecting precursors of failure with Sentinel-1 data". *Landslides*, Vol. 15, 2018, pp. 123-133. https://doi.org/10.1007/s10346-017-0915-7

[12] A. Barra, L. Solari, M. Béjar-Pizarro, O. Monserrat, S. Bianchini, G. Herrera & al, "A methodology to detect and update active deformation areas based on Sentinel-1 SAR images". *Remote Sensing*, Vol. 9, Issue. 10, no. 1002, 2017, https://doi.org/10.3390/rs9101002

[13] F. D. Van der Meer, H.M.A. Van der Werff, F.J.A. Van Ruitenbeek, C.A. Hecker, W.H. Bakker, M.F. Noomen, M. Van der Meijde, E.J.M. Carranza, J. Boudewijn de Smeth & T. Woldai, "Multi- and hyperspectral geologic remote sensing: A review", *International Journal of Applied Earth Observation and Geoinformation*, Vol. 14, Issue 1, 2012, pp. 112-128.

[14] A. Foucault, J.F. Raoult, "Dictionary of geology", 4th edition, Elsevier Masson, 1997, pp. 324.

[15] L. Asebriy, A. Azdimmousa, and J. Bourgois, "Structure du Rif externe sur la transversale du Massif de Kétama," Travaux de l'Institut Scientifique, Série Géologie & Géographie physique, (Rabat, Morocco), no. 21, Feb. 2003, pp. 27-46.

[16] R. Bürgmann, P.A. Rosen & E. J. Fielding, "Synthetic aperture radar interferometry to measure Earth's surface topography and its deformation", *Annual review of earth and planetary sciences*, Vol. 28, 2000, pp. 169-209.

[17] M. Simons & P.A. Rosen, "Interferometric Synthetic Aperture Radar Geodesy". In: Gerald Schubert (editor-in-chief) Treatise on Geophysics, 2nd edition, Vol. 3, Oxford: Elsevier; 2015. pp. 339-385.

[18] A. Augier, "Interférométrie radar : principes et utilisation dans la surveillance de la déformation du sol", Planet Terre - ISSN 2552-9250, January. 2020, https://planet-terre.ens-lyon.fr/ressource/interferometrie-radar.xml

[19] A. Moreira, P. Prats-Iraola, M. Younis, G. Krieger, I. Hajnsek & K. P. Papathanassiou, "A tutorial on synthetic aperture radar", *IEEE Geoscience and Remote Sensing Magazine*, vol. 1, no. 1, March 2013, pp. 6-43, doi: 10.1109/MGRS.2013.2248301.

[20] RB. Lohman & M. Simons, "Some thoughts on the use of InSAR data to constrain models of surface deformation: Noise structure and data downsampling", *Geochemistry, Geophysics, Geosystems*, Vol. 6, Issue. 1, 2005. p.p 12.

[21] F. Cigna, L.B. Bateson, C.J. Jordan & C. Dashwood, "Simulating SAR geometric distortions and predicting Persistent Scatterer densities for ERS-1/2 and ENVISAT C-band SAR and InSAR applications: Nationwide feasibility assessment to monitor the landmass of Great Britain with SAR imagery". *Remote Sensing of Environment*, Vol. 152, 2014, pp. 441-466.

[22] K. Dai, Z. Li, R. Tomás, G. Liu, B. Yu, X. Wang & al, "Monitoring activity at the Daguangbao mega-landslide (China) using Sentinel-1 TOPS time series interferometry". *Remote Sensing of Environment*, Vol. 186, 2016, pp. 501-513.

[23] F. J. Meyer, "Sentinel-1 InSAR Processing using the Sentinel-1 Toolbox," In: Adapted from. Coursework developed in Alaska Satellite Facility, version 5.4, June. 2019. https://asf.alaska.edu/wp-content/uploads/2019/05/generate_insar_with_s1tbx_v5.4.pdf OK

[24] Serco Italia SPA (2020). "Rapid Landslide Detection with Sentinel-1". Retrieved from RUS Copernicus Project Lectures, European Space Agency, March 2020, version 1.1. https://rus-copernicus.eu/portal/the-rus-library/learn-by-yourself/

[25] M. Hamidi, T. Bouramtane, S. Abraham, I. Kacimi, L. Barbiero, N. Kassou, & al. 2023. "Landslide Hazard Assessment in the Heterogeneous Geomorphological and Environmental Context of the Rif Region, Morocco – A Machine Learning Approach". *Ecological Engineering & Environmental Technology*, Vol. 24, No. 8, 2023, pp. 272-292. https://doi.org/10.12912/27197050/172569

[26] B. Taj, M. Mastere, B. Benzougagh, M. El Hilali, S. Sassioui & B. El Fellah, "Geotechnical Prospects and Electrical Tomography to Study Slope Instability in the Rif Alboran Sea Shoreline on The Mediterranean By-Road (Northern Morocco)". *Ecological Engineering & Environmental Tech*nology, Vol. 25, No. 1, 2024, pp. 138-151. https://doi.org/10.12912/27197050/174340

[26] P. Aleotti, R. Chowdhury. "Landslide hazard assessment: summary review and new perspectives". *Bulletin of Engineering Geology and the Environment,* Vol. 58, 1999, pp. 21-44. https://doi.org/10.1007/s100640050066